Non-linear programming applied to finite element lower bound limit analysis in soil mechanics

T. AKHLAGHI
Department of Civil Engineering
Islamic Azad University – Salmas Branch
Jomhori Islami Boulevard, PO Box 58815-386, Salmas
IRAN

Abstract: The non-linear programming theory along with active set algorithm is employed to solve the objective function of quadratic type problem in soil mechanics under plain strain and two dimensional loading conditions. Combination of lower bound limit analysis and finite element method leads to an appropriate procedure for determining the collapse load of the system. In this combined method, a linear approximation of yield surface is used and by applying the equilibrium, stress boundary and discontinuity condition and utilizing a suitable optimization technique, the statically admissible stress field is obtained from which a lower safe limit to collapse load is computed. In order to assess the usefulness of the proposed technique, a number of examples are given and the results obtained from this technique are compared with the published results on those examples. Based on the comparisons made, the accuracy and efficiency of the method are examined and discussed.

Key-Words: Lower bound limit, Non-linear programming, Soil mechanics

1 Introduction

The lower bound theorem of classical plasticity theory is a powerful tool for the analysis of stability problems in soil mechanics. The theory assumes a perfectly plastic soil model with an associated flow rule and states that any statically admissible stress field will furnish a lower bound estimate of the true limit load.

Although the lower bound theorem is a particularly useful tool, however, it is often difficult to apply to practical problems involving complicated loading and complex geometry. An alternative method of computing lower bounds, which uses finite elements and linear or nonlinear programming has been presented by Lysmer(1970) and Sloan(1988) for linear case and by Modarres-Motlagh(1997) and Lyamin and Sloan(2002) for nonlinear one.

A major advantage of the numerical formulation of lower bound theorem is that complex loading and geometries can be dealt with. The principle disadvantage of technique is that significant amounts of computation time may be necessary to solve the resultant programming problem especially if the traditional simplex or revised simplex algorithms are used. This is because the approximated yield criterion typically generates a very large number of inequality constraints on the nodal stresses. Sloan(1988) overcame this problem by employing an active set algorithm to solve linear programming problem. Moreover he improved this algorithm by using factorization and updating strategy, that has been expressed by Reid(1976). For this purpose Modarres-Motlagh(1997) employed a convex quadratic active set algorithm and Reid's factorization and updating strategy and solved a quadratic programming for determining lower bound of collapse load in mechanical component.

In this paper, a convex quadratic active set algorithm is employed to solve the quadratic programming problem in soil mechanics under plain strain condition and 2-D loading. To illustrate the effectiveness of procedure, a number of footing problems are analyzed and the results are compared with known exact solutions obtained by other researchers.

2 Finite Element Formulation of the Lower Bound Theorem

The finite element formulation of the lower bound theorem followed uses three nodded triangular stress elements, according to Sloan (1988). Each node is associated with three stresses σ_x, σ_y and τ_{xy} (Fig. 1). The variation of stresses throughout each element is assumed to be linear based on the following equations:

$$\sigma_x = \sum_{i=1}^{3} N_i \sigma_{xi} \quad ; \quad \sigma_y = \sum_{i=1}^{3} N_i \sigma_{yi} \quad ; \quad \tau_{xy} = \sum_{i=1}^{3} N_i \tau_{xyi} \quad (1)$$

where σ_{xi}, σ_{yi}, and τ_{xyi} are the nodal stresses and N_i are the linear shape functions. The shape functions are given by:

$$N_1 = \frac{\xi_1 + \eta_1 x + \zeta_1 y}{2A} \quad ; \quad N_2 = \frac{\xi_2 + \eta_2 x + \zeta_2 y}{2A} \quad ;$$
$$N_3 = \frac{\xi_3 + \eta_3 x + \zeta_3 y}{2A} \qquad (2)$$

where $\xi_1 = x_2 y_3 - x_3 y_2$; $\eta_1 = y_2 - y_3$; $\zeta_1 = x_3 - x_2$

$\xi_2 = x_3 y_1 - x_1 y_3$; $\eta_2 = y_3 - y_1$; $\zeta_2 = x_1 - x_3$

$\xi_3 = x_1 y_2 - x_2 y_1$; $\eta_3 = y_1 - y_2$; $\zeta_3 = x_2 - x_1$

$2A$ is equal to twice the element area and is expressed by: $2A = |\eta_1 \zeta_2 - \eta_2 \zeta_1|$

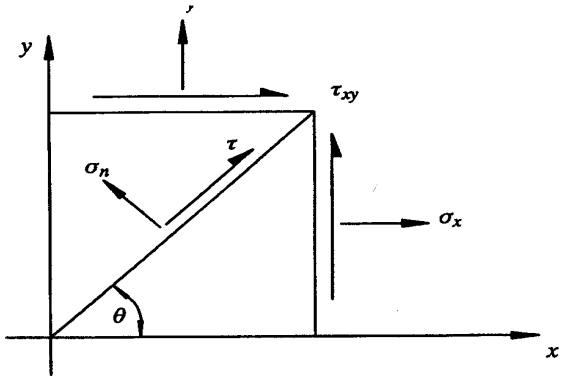

Fig.1: Resolution of stresses into normal and shear components

Unlike the elements used in displacement finite element analysis, several nodes may share the same coordinate with each node associated with only one element. In this way statically admissible stress discontinuities can occur at all edges between adjoining triangles. By ensuring that the equations of equilibrium are satisfied, and that the stress boundary conditions and the yield criterion are not violated, a rigorous lower bound on the collapse load is obtained.

2.1 Element Equilibrium

With the sign convention of Fig. 2 the stresses throughout each element must satisfy the following two equations in order to ensure equilibrium:

$$\frac{\partial \sigma_x}{\partial x} + \frac{\partial \tau_{xy}}{\partial y} = 0 \quad ; \quad \frac{\partial \sigma_y}{\partial y} + \frac{\partial \tau_{xy}}{\partial x} = \gamma \qquad (3)$$

Where tensile stresses are taken positive, a right handed Cartesian coordinate system is adopted and γ is the unit weight of the soil. Given that the stress field varies linearly across each element, according to

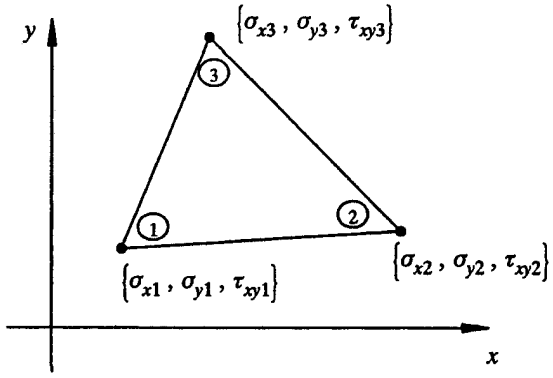

Fig. 2: Three-nodded linear stress triangle

Eqs. (1)-(3), we can derive the following equality constraints on the nodal stresses for each element:

$$[A_{eq}]\vec{x} = \vec{b}_{eq} \qquad (4)$$

where:

$$[A_{eq}] = \frac{1}{2A_e}\begin{bmatrix} \xi_1 & 0 & \eta_1 & \xi_2 & 0 & \eta_2 & \xi_3 & 0 & \eta_3 \\ 0 & \eta_1 & \xi_1 & 0 & \eta_2 & \xi_2 & 0 & \eta_3 & \xi_3 \end{bmatrix}$$

$$\vec{x}^T = \{\sigma_{x1}, \sigma_{y1}, \tau_{xy1}, \sigma_{x2}, \sigma_{y2}, \tau_{xy2}, \sigma_{x3}, \sigma_{y3}, \tau_{xy3}\}$$

$\vec{b}_{eq}{}^T = \{0, \gamma\}$ and A_e = area of element

2.2 Admissible Stress Discontinuity Equilibrium

For a discontinuity to be statically admissible only the tangential component of stress may be discontinuous, with continuity of the corresponding shear and normal stresses maintained. With reference to Fig. 1, the normal and shear stresses acting on a plane inclined at angle θ to the x-axis (positive anti-clockwise) are given by:

$$\sigma_n = \sin^2\theta\sigma_x + \cos^2\theta\sigma_y - \sin 2\theta\tau_{xy}$$
$$\tau = -\frac{1}{2}\sin 2\theta\sigma_x + \frac{1}{2}\sin 2\theta\sigma_y + \cos 2\theta\tau_{xy} \qquad (5)$$

Looking at Fig. 3, for triangles a and b, equilibrium along the discontinuity requires that at every point along this side:

$$\sigma_n^a = \sigma_n^b \quad ; \quad \tau^a = \tau^b \qquad (6)$$

Since stresses are confined to varying linearly along any element edge, an equivalent condition is achieved by enforcing the constraints:

$$\sigma_{n1}^a = \sigma_{n2}^b \; ; \; \sigma_{n3}^a = \sigma_{n4}^b \; ; \; \tau_1{}^a = \tau_2{}^b \; ; \; \tau_3{}^a = \tau_4{}^b \qquad (7)$$

Substituting into Eq. (6) leads to:

$$[A_{dis}]\vec{x} = \vec{b}_{dis} \qquad (8)$$

where : $[A_{dis}]=\begin{bmatrix} T & -T & 0 & 0 \\ 0 & 0 & T & -T \end{bmatrix}$

and

$$[T]=\begin{bmatrix} \sin^2\theta_d & \cos^2\theta_d & -\sin 2\theta_d \\ -\frac{1}{2}\sin 2\theta_d & \frac{1}{2}\sin 2\theta_d & \cos 2\theta_d \end{bmatrix}$$

$$\vec{x}^T=\{\sigma_{x1},\sigma_{y1},\tau_{xy1},\sigma_{x2},\sigma_{y2},\tau_{xy2},\sigma_{x2},\sigma_{y3},\tau_{xy3},\sigma_{x4},\sigma_{y4},\tau_{xy4}\}$$

$$\vec{b}_{dis}{}^T=\{0,0,0,0\}$$

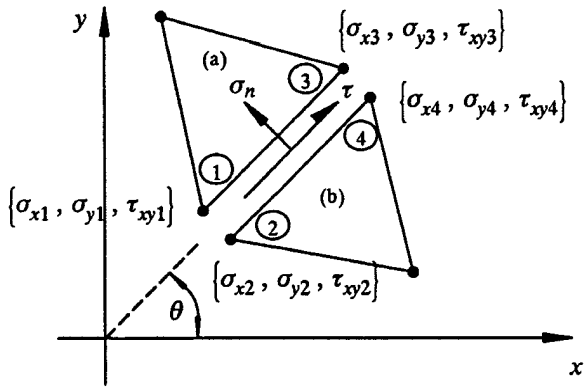

Fig. 3: Statically admissible stress discontinuity

As such, each statically admissible discontinuity along an element edge produces four equality constraints on the nodal stresses.

2.3 Boundary Conditions

In order to enforce prescribed boundary conditions, it is necessary to impose additional constraints on the nodal stresses. The problem of a wall under combined normal and shear load has boundary conditions of the form:

$$\sigma_n^l = q = constant \;\; ; \;\; \tau^l = t = constant \qquad (9)$$

Given a linear variation of the stress components σ_x, σ_y and τ_{xy} along the edge of each triangle, a more general boundary condition may be imposed of the form:

$$\sigma_n^l = q_1 + (q_2 - q_1)\xi \;\; ; \;\; \tau^l = t_1 + (t_2 - t_1)\xi \qquad (10)$$

where l is the triangle edge where boundary tractions are specified; ξ is the local coordinate along l; q_1 and q_2 are the normal stresses specified at nodes 1 and 2 (tension positive); t_1 and t_2 are the shear stresses specified at nodes 1 and 2 (clockwise shears considered positive), as shown in Fig. 4.

The boundary conditions of Eq. (9) are then satisfied by requiring:

$$\sigma_{n1} = q_1 \;\; ; \;\; \sigma_{n2} = q_2 \;\; ; \;\; \tau_1 = t_1 \;\; ; \;\; \tau_2 = t_2 \qquad (11)$$

If θ_l is the angle of side l to the positive x axis (measured positive anti-clockwise), then using Eq. (6), the stress boundary conditions result in the equality constraints:

$$[A_{bound}]\vec{x} = \vec{b}_{bound} \qquad (12)$$

where: $[A_{bound}]=\begin{bmatrix} T & 0 \\ 0 & T \end{bmatrix}$ and

$$[T]=\begin{bmatrix} \sin^2\theta_l & \cos^2\theta_l & -\sin 2\theta_l \\ -\frac{1}{2}\sin 2\theta_l & \frac{1}{2}\sin 2\theta_l & \cos 2\theta_l \end{bmatrix} \;\; ;$$

$$\vec{x}^T=\{\sigma_{x1},\sigma_{y1},\tau_{xy1},\sigma_{x2},\sigma_{y2},\tau_{xy2}\} \;\; ;$$

$$\vec{b}_{bound}{}^T=\{q_1,t_1,q_2,t_2\}$$

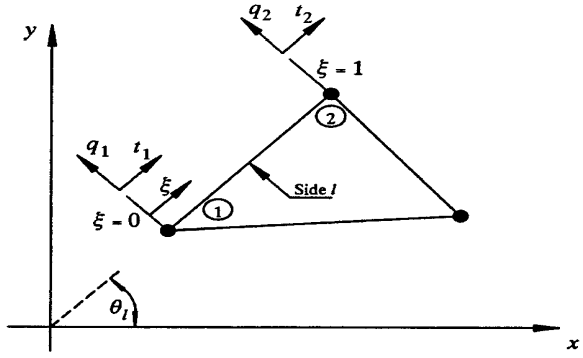

Figure 4. Stress boundary conditions

And so for each edge where boundary traction is specified, a maximum of four equality constraints on the nodal stresses are generated.

2.4 Yield Condition

Assuming tensile stresses are taken as positive and plain strain conditions, the Mohr-Coulomb yield criterion may be expressed as:

$$F=(\sigma_x-\sigma_y)^2+(2\tau_{xy})^2-(2c\cos\phi-(\sigma_x+\sigma_y)\sin\phi)^2=0 \qquad (13)$$

since that the stresses should not violate the yield condition, and hence fulfill the requirements of the lower bound theorem, it is necessary that $F \le 0$ throughout each triangle. Since we wish to formulate the lower bound theorem as a linear or quadratic programming problem, it is required to approximate equation (13) by a yield criterion which is a linear function of the unknown stresses. To ensure that the solution obtained is a strict lower bound on the exact collapse load, the linearized yield surface must lie inside the Mohr-Coulomb yield surface in stress space.

Letting:

$$X=\sigma_x-\sigma_y \;;\; Y=2\tau_{xy} \;;\; R=2c\cos\phi-(\sigma_x+\sigma_y)\sin\phi \qquad (14)$$

The Mohr-Coulomb yield function may be written as $X^2 + Y^2 = R^2$. In terms of the variables X and Y, this plots as a circle as shown in Fig. 5. The Mohr-Coulomb yield surface is approximated by an interior polygon with p_1 sides and p_1 vertices. In general the linearized yield surface is given by:

$$A_k\sigma_x + B_k\sigma_y + C_k\tau_{xy} \le D \;\; ; \;\; k = 1,2,..., p_1 \qquad (15)$$

where for Mohr-Coulomb yield surface:

$$A_k = \cos\frac{2\pi k}{p_1} + \sin\phi\cos\frac{\pi}{p_1} \; ; \;\; C_k = 2\sin\frac{2\pi k}{p_1} \qquad (16)$$

$$B_k = -\cos\frac{2\pi k}{p_1} + \sin\phi\cos\frac{\pi}{p_1} \; ; \;\; D = 2c\cos\phi\cos\frac{\pi}{p_1}$$

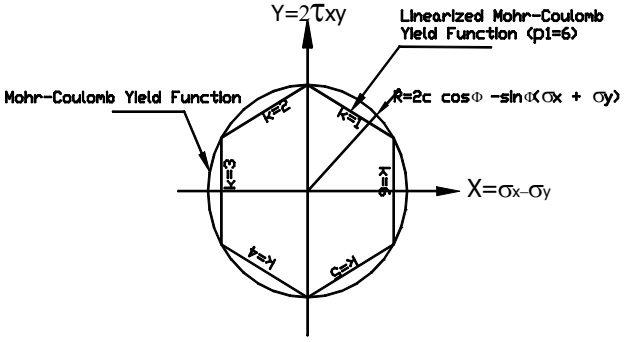

Fig.5: Linearized Mohr-Coulomb yield function

The constraints imposed on the stresses at each node due to linearized yield criterion may be summarized by the matrix equation:

$$\left[A_{yield}\right]\vec{x} \le \vec{b}_{yield} \qquad (17)$$

where:

$$\left[A_{yield}\right] = \begin{bmatrix} A_1 & B_1 & C_1 \\ A_2 & B_2 & C_2 \\ . & . & . \\ . & . & . \\ . & . & . \\ A_{p_1} & B_{p_1} & C_{p_1} \end{bmatrix}_{p\times 3}$$

$$\vec{x}^T = \{\sigma_x, \sigma_y, \tau_{xy}\} \quad ; \quad \vec{b}_{yield}{}^T = \{D_1, D_2, ..., D_{p_1}\}$$

Hence the linearized yield condition generates p_1 inequality constraints on each nodal stress vector. Since there are *3E* nodes for a mesh of *E* triangles, the total number of inequality constraints generated is $3p_1E$.

2.5 Objective Function

For most plain strain geotechnical problems, if unknown external loads are applied normal to element boundary side, it is wished to find statically admissible stress field which maximizes an integral of the form:

$$Q = h\int_s \sigma_n ds \qquad (18)$$

where Q is the collapse load, h is the out of plane thickness, and σ_n is the normal stress acting over some part of the boundary *s*. Fig. 6 illustrates an edge of triangle, defined by nodes 1 and 2. Since the stresses are assumed to vary linearly throughout each element, Q is given by:

$$Q = \frac{lh}{2}(\sigma_{n1} + \sigma_{n2}) \qquad (19)$$

where l is the length of the edge *s* and σ_{n1}, σ_{n2} are the normal stresses at nodes 1 and 2 of triangle *e*.

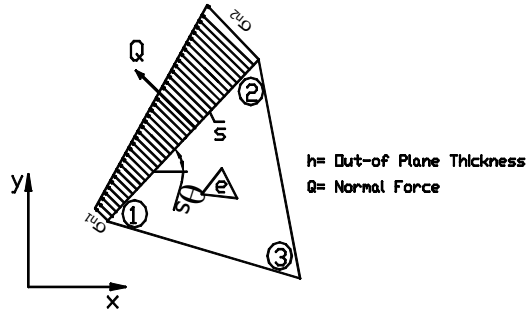

Fig. 6: Load in a direction normal to the boundary edge

If unknown external load is only in a direction tangential to boundary edge (Fig. 7), as above, Q is given by:

$$Q = \frac{lh}{2}(\tau_1 + \tau_2) \qquad (20)$$

where τ_1 and τ_2 are the shear stresses at nodes 1 and 2 of triangle *e*.

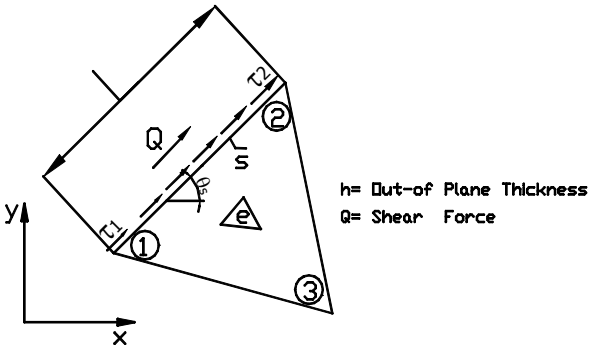

Fig. 7: Load in a direction tangential to the boundary edge

If external loading is in the direction of both normal and tangential to the boundary edge, according to Eqs. (19) and (20), the collapse load to be maximized is given by:

$$Q^2 = Q_x{}^2 + Q_y{}^2 \qquad (21)$$

where:

$$Q_x = \sum_s \frac{l_l h_i}{2}(\sigma_{n1} + \sigma_{n2})\sin\theta_s + \sum_s \frac{l_i h_i}{2}(\tau_1 + \tau_2)\cos\theta_s$$

$$Q_y = \sum_s \frac{l_l h_i}{2}(\sigma_{n1} + \sigma_{n2})\cos\theta_s + \sum_s \frac{l_i h_i}{2}(\tau_1 + \tau_2)\sin\theta_s$$

In order to formulation of collapse load (Q) due to nodal stresses σ_x, σ_y and τ_{xy}; Eqs. (5) and (21) are combined and give:

$$Q^2 = Q_x{}^2 + Q_y{}^2 = \{\sigma\}^T H \{\sigma\} \qquad (22)$$

where:

$$Q_x = C_1\sigma_{x1} + C_2\sigma_{y1} + C_3\tau_{xy1} + \ldots + C_{n-2}\sigma_{xN} + C_{n-1}\sigma_{yN} + C_n\tau_{xyN}$$

$$Q_y = CC_1\sigma_{x1} + CC_2\sigma_{y1} + CC_3\tau_{xy1} + \ldots + CC_{n-2}\sigma_{xN} + CC_{n-1}\sigma_{yN} + CC_n\tau_{xyN}$$

H is symmetric Hessian matrix, and CC_i are unknown external load components in x and y direction respectively, which are functions of θ_s, l_i and h_i.

Generally, in order to solving both linear and quadratic programming problems, the objective function is written in the form of:

$$Q = C^T\{\sigma\} + \frac{1}{2}\{\sigma\}^T H \ \{\sigma\} \qquad (23)$$

where C is the coefficient of linear part of the objective function. For example, if external loading acts only normal to the boundary side s, by assuming unit thickness in the out-of-plane direction, the coefficient vector C is given by:

$$\{C^s\}^T = \frac{l}{2}\{\sin^2\theta_s, \cos^2\theta_s, -\sin 2\theta, \sin^2\theta_s, \cos^2\theta_s, -\sin 2\theta_s\}$$

3 Application

To illustrate the usefulness and effectiveness of the procedure described above, a number of footing examples are analyzed and the results obtained are compared with other researcher's finding and known exact solutions. The selected problems are those given and solved by Sloan(1988), so that the results of this study can be easily compared with his available results.

3.1 Undrained Loading of Smooth Strip Footing

This problem and the meshes used to analyze the problem are shown in Fig. 8 and the results are summarized in Table 1 for various values of p_1 (the number of sides in linearized yield polygon).

The Meyerhof solution for this problem gives the exact collapse pressure (bearing capacity) as $q = N_c c_u i_c$, where c_u is the undrained shear strength, i_c is the inclination factor defined as $i_c = (1 - \frac{\alpha^\circ}{90})^2$, where α is the angle between load and vertical direction and $N_c = 2 + \pi = 5.14$ from Prandtl solution.

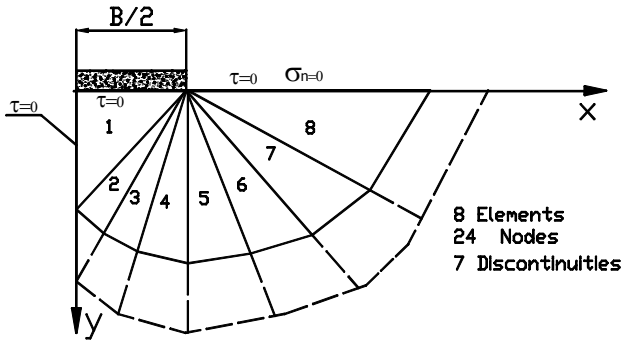

Fig. 8: Meshes for smooth strip footing on purely cohesive soil ($\phi = 0$, $c = 1$)

Table 1: Results for smooth rigid footing on a purely cohesive soil ($\phi = 0$, $c = 1$)

p_1	N_c Proposed Solution	N_c Sloan Solution	N_c Exact	Proposed Solution Iteration Number	Sloan Iteration Number	Proposed Solution Run time (sec)	Sloan Run time (sec)
6	4.66	4.72	5.14	11	40	0.1	0.5
12	5.04	5.03	5.14	12	58	0.2	0.7
24	5.09	5.06	5.14	11	85	0.5	1.4
48	5.10	5.07	5.14	24	125	1.0	2.9
48*	5.10	5.08	5.14	23	210	1.0	4.2

*results for extended mesh

3.2 Drained Loading of Smooth Strip Footing

This problem and the meshes used to analyze the problem are shown in Fig. 9 and the results are summarized in Table 2 for various values of p_1.

The exact bearing capacity for a smooth strip footing resting on a cohesive-frictional soil may be written as:

$$q = cN_c i_c + qN_q i_q$$

where: $N_q = \exp(\pi\tan\phi)\tan^2(\frac{\pi}{4} + \frac{\phi}{2})$; $N_c = (N_q - 1)\cot\phi$;

q is the overburden pressure and i_c and i_q are the inclination factors. For the case of a surface footing we have:

$$N_q = \frac{q}{c\, i_c \cot\phi} + 1$$

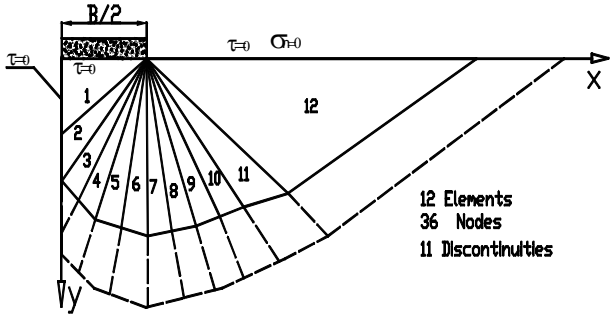

Fig. 9: Meshes for smooth strip footing on a cohesive-frictional soil ($\phi = 40$, $c = 1$)

Table 2: Results for smooth rigid footing on a cohesive-frictional soil ($\phi = 40$, $c = 1$)

p_1	N_q Proposed Solution	N_q Sloan Solution	N_q Exact	Proposed Solution Iteration Number	Sloan Iteration Number	Proposed Solution Run time (sec)	Sloan Run time (sec)
6	55.52	35.68	64.2	16	112	0.2	1.6
12	61.84	53.58	64.2	20	156	0.5	2.6
24	63.47	59.69	64.2	34	219	1.0	4.6
48	63.90	61.35	64.2	51	421	1.5	12.5
48*	63.75	61.11	64.2	49	404	1.5	11.4

*results for extended mesh

4 Conclusions

In this paper a new combined method based on finite elements and lower bound limit analysis is used to determine the lower bound for bearing capacity of surface footing under two dimensional loading. By solving these problems the nondimensional factors N_q and N_c are computed and compared with exact values of these factors. The comparison of the results shows that the values of these factors obtained using the proposed method are closer to the exact value than the Sloan(1988) solution and also the iteration number and computer run time spent to solve the problems using this method are less than that using Sloan's method. This is because of employing the convex quadratic active set algorithm along with factorization and updating strategy which have been used in the developed algorithm during this research work and promising that the developed method is a useful technique for determining the collapse load of engineering problems.

References:

[1] Augarde, C. E., Lyamin, A. V., and Sloan, S. W., Stability of Undrained Plane Strain Heading Revisited, *International Journal of Computers and Geotechnics,* Vol.30, 2001, pp. 419-430.

[2] Carter, J. P., Booker, J. R., and Zheng, X., Limit Analysis of Bearing Capacity of Fissured Materials, *International Journal of Solids and Structures*, Vol.37, 2001, pp. 1211-1243.

[3] Lysmer, J., Limit Analysis of Plane Problem in Soil Mechanics, *Journal of Soil Mechanics Foundation Division, ASCE*, Vol.96(SM4), 1970, pp. 1311-1334.

[4] Lyamin, A.V., and Sloan, S. W., Lower Bound Limit Analysis using Finite Elements and Nonlinear Programming, *International Journal for Numerical Methods in Engineering*, Vol.55(5), 2002, pp. 573-611.

[5] Lyamin, A.V., and Sloan, S. W., Mesh Generation for Lower Bound Limit Analysis, *International Journal of Advances in Engineering Software*, Vol.34, 2003, pp. 321-338.

[6] Modarres-Motlagh, A., *Lower Bound to Collapse Load for Structures*, Ph D Thesis, University of NSW, Australia, 1997.

[7] Reid, J. K., *FORTRAN subroutines for handling sparse linear programming bases*, Harwell Report, A.E.R.E., R8269, 1976.

[8] Sloan, S. W., Lower Bound Limit Analysis Using Finite Element and Linear Programming, *International Journal of Analytical Methods in Geomechanics,* Vol.12, 1988, pp. 61-77.

[9] Sloan and Booker, J. R., Integration of Tresca and Mohr-Coulomb Constitutive Relation in Plane Strain Elastoplasticity, *International Journal for Computer and Structures*, Vol.65, 1992, pp. 890-906.

[10] Sutcliffe, H. S., and Page, A. W., Lower Bound Limit Analysis of Unreinforced Masonary Shear Walls, *International Journal for Computers and Structures*, Vol.79, 2001, pp. 1295-1342.